Nematic Susceptibility of Hole-Doped and Electron-Doped $BaFe_2As_2$ Iron-Based Superconductors from Shear Modulus Measurements

A. E. Böhmer,[1,2,*] P. Burger,[1,2] F. Hardy,[1] T. Wolf,[1] P. Schweiss,[1] R. Fromknecht,[1] M. Reinecker,[3] W. Schranz,[3] and C. Meingast[1,†]

[1]*Institut für Festkörperphysik, Karlsruhe Institute of Technology, 76021 Karlsruhe, Germany*
[2]*Fakultät für Physik, Karlsruhe Institute of Technology, 76131 Karlsruhe, Germany*
[3]*Faculty of Physics, University of Vienna, Boltzmanngasse 5, Vienna A-1090, Austria*

(Received 15 May 2013; revised manuscript received 4 October 2013; published 28 January 2014)

The nematic susceptibility, χ_φ, of hole-doped $Ba_{1-x}K_xFe_2As_2$ and electron-doped $Ba(Fe_{1-x}Co_x)_2As_2$ iron-based superconductors is obtained from measurements of the elastic shear modulus using a three-point bending setup in a capacitance dilatometer. Nematic fluctuations, although weakened by doping, extend over the whole superconducting dome in both systems, suggesting their close tie to superconductivity. Evidence for quantum critical behavior of χ_φ is, surprisingly, only found for $Ba(Fe_{1-x}Co_x)_2As_2$ and not for $Ba_{1-x}K_xFe_2As_2$—the system with the higher maximal T_c value.

DOI: 10.1103/PhysRevLett.112.047001 PACS numbers: 74.25.Ld, 74.40.Kb, 74.62.Fj, 74.70.Xa

As in many other unconventional superconductors, superconductivity in iron-based superconductors arises close to the point where an antiferromagnetic spin-density-wave transition (SDW) is suppressed [1,2]. A particular feature of the iron-based materials is that the SDW breaks the fourfold rotational symmetry of the lattice which is accompanied by an orthorhombic distortion [2]. The fact that the structural transition surprisingly precedes the SDW transition in some systems has led to a strong debate about the driving force of the structural phase transition; e.g., orbital [3–5] or spin-nematic [6,7] degrees of freedom have been proposed. Importantly, orbital and spin fluctuations are also likely candidates for the superconducting pairing glue [8,9]. Whereas spin fluctuations are believed to mediate $s_\pm$ superconductivity [8,10,11], orbital fluctuations are thought to lead to s_{++} superconductivity [5,9]. The structural transition in the Fe-based materials is of strong current interest [7,12–16], because it is believed to be of an electronic nematic type, i.e., a transition in which a "nematic" order parameter of electronic (e.g., spin or orbital) origin causes a spontaneous breaking of the fourfold lattice symmetry. Such nematic transitions are believed to occur also in $Sr_3Ru_2O_7$ and the cuprate superconductors [17,18].

Measurements of the elastic shear modulus C_{66}, which is the soft mode of the structural transition, provide a powerful tool for studying the susceptibility and associated fluctuations of this nematic order parameter [19–21]. In particular, the softening of C_{66} was studied intensively in $Ba(Fe_{1-x}Co_x)_2As_2$ (Co-Ba122) using ultrasound, and strong evidence for a quantum critical point (QCP) was obtained near optimal doping [21]. Further, the response of C_{66} below the superconducting transition at T_c provides important information about the coupling of these fluctuations to superconductivity, which has been interpreted both in the spin-nematic and the orbital scenario [19,21]. Up to the present, shear-modulus data have only been reported for the electron-doped Co-Ba122 system from ultrasound measurements. It is clearly of interest to establish whether the nematic susceptibility of other Fe-based superconductors shows similar behavior.

In this Letter we present an extensive study of the nematic susceptibility derived from shear modulus data of both hole-doped $Ba_{1-x}K_xFe_2As_2$ (K-Ba122) and electron-doped Co-Ba122 covering a wide doping range. We find that nematic fluctuations are enhanced over the whole superconducting dome of both systems, suggesting their close tie to superconductivity. Surprisingly, evidence for quantum critical behavior of the nematic susceptibility is only found for Co-Ba122, and not for K-Ba122—the system with the higher maximal superconducting transition temperature $T_{c,\max}$.

Self-flux grown single crystals of Co-Ba122 and K-Ba122 were cut to dimensions of $L \times w \times h \sim (2-3 \times 1 \times 0.1)$ mm^3 [see Fig. 1(b)]. We gain access to their shear modulus C_{66} via a measurement of the Young's modulus (i.e., the modulus of elasticity for uniaxial tension) along the tetragonal [110] direction $Y_{[110]}$, using the novel technique of a three-point bending setup in a capacitance dilatometer [22,23] [see Figs. 1(a) 1(b)]. If C_{66} is small, it is expected to dominate $Y_{[110]}$ [23,24]. This certainly holds close the structural transition, but, as we demonstrate on the Co-Ba122 system, our method yields very similar results as the ultrasound data over the whole doping range [21], showing that the temperature dependence of C_{66} may be reliably obtained also by three-point bending. Figures 1(c) 1(d), show the Young's modulus $Y_{[110]}/Y_{[110]}(293\ \mathrm{K})$ of Co-Ba122 and K-Ba122, which was normalized at room temperature because of uncertainties in the geometrical parameters L, w, and h. Importantly, our data on Co-Ba122 agree very well with the C_{66} results of Ref. [21] over the

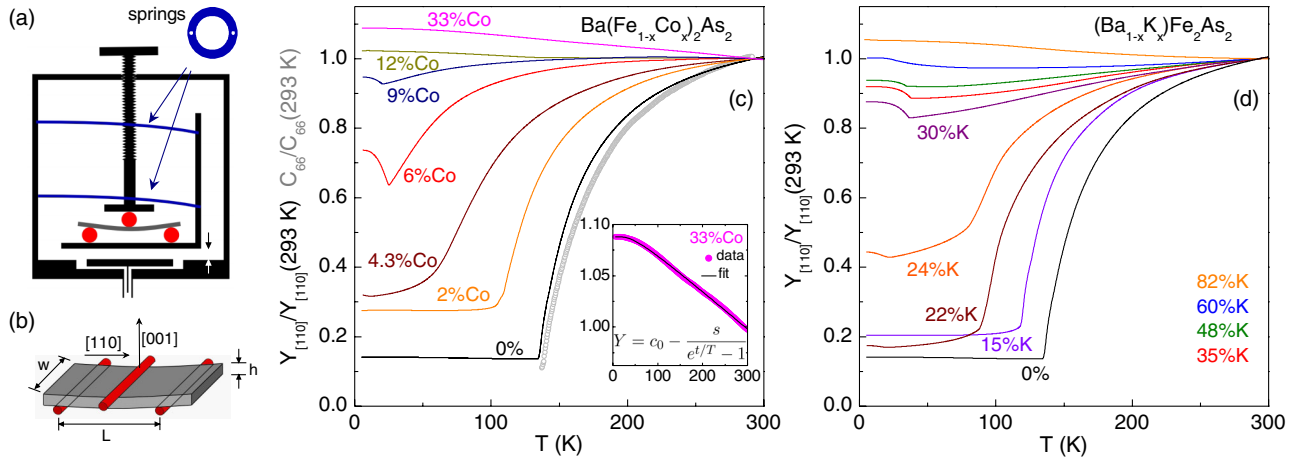

FIG. 1 (color online). (a) Schematic drawing of our three-point-bending setup in the capacitance dilatometer. The sample (gray) is supported by three wires (red) and the capacitor gap is indicated by small arrows. (b) Definition of sample dimensions and orientation relative to the wire supports. Young's modulus $Y_{[110]}$ of (c) Co-Ba122 and (d) K-Ba122, normalized at room temperature. For comparison, the temperature dependence of the C_{66} mode of pure $BaFe_2As_2$ from Ref. [21] (gray circles) is shown in (c). The inset in (c) shows a fit of the data of the 33% Co-Ba122 sample to the Varshni formula used as the phonon background.

whole doping range; for a direct comparison we have also plotted C_{66} data for $x = 0$ in Fig. 1(c).

Both characteristics of the electron-doped system, namely, the softening on approaching the structural transition at T_s from above and the hardening below T_c, are observed also in hole-doped K-Ba122. However, the softening and subsequent hardening, at, e.g., optimal doping, is much more pronounced for Co than for K doping, which will be discussed in more detail later.

In general, the elastic constants associated with the soft mode are expected to go to zero at a second-order structural phase transition and to harden below [25]. Surprisingly, this is not the case here and $Y_{[110]}$, even though it decreases by 50%–85%, never reaches zero, a behavior which is not fully understood and also observed in ultrasound data [21]. Also, we find that T_s manifests itself as a kink in $Y_{[110]}(T)$ and that $Y_{[110]}$ stays soft, or even grows softer below T_s, contrary to the general expectation. This effect presumably arises from "superelastic" behavior [26,27], i.e., from the motion of boundaries between structural twins that are formed in the orthorhombic phase.

As argued previously [15,28], the structural transition in Ba122 is most likely driven by an electronic order parameter φ via bilinear coupling to the orthorhombic strain $\varepsilon_6 = (a-b)/(a+b)$. ($a$ and b are the in-plane lattice constants in the orthorhombic phase.) In this case, the Landau expansion of the free energy is given by

$$F = \frac{1}{2}(\chi_\varphi)^{-1}\varphi^2 + \frac{B}{4}\varphi^4 + \frac{C_{66,0}}{2}\varepsilon_6^2 - \lambda\varphi\varepsilon_6, \qquad (1)$$

where λ is the electron-lattice coupling constant and $C_{66,0}$ the bare elastic constant, which has no strong temperature dependence and B is the quartic coefficient of the Landau expansion. Bilinear coupling is allowed because φ and ε_6 both break the same fourfold rotational symmetry. We therefore refer to φ as the nematic order parameter with χ_φ the associated nematic susceptibility. φ may represent, e.g., the spin-nematic or the orbital order parameter; however, the present thermodynamic treatment cannot distinguish between these scenarios. C_{66} is renormalized due to the coupling λ [19,25,29], and is given by

$$C_{66} = C_{66,0} - \lambda^2\chi_\varphi. \qquad (2)$$

At a mean field level, the temperature dependence of χ_φ is given by $\chi_\varphi = [A(T - T_0)]^{-1}$, reflecting that χ_φ diverges at the "bare" transition temperature T_0, i.e., the nematic ordering temperature in the absence of electron-lattice coupling. Because of the coupling λ, however, the ordering of φ and the associated structural distortion takes place at $T_s^{\mathrm{CW}} = T_0 + \lambda^2/AC_{66,0}$, the temperature at which χ_φ reaches the critical value $C_{66,0}/\lambda^2$. C_{66} in turn follows the modified Curie-Weiss law

$$\frac{C_{66}}{C_{66,0}} = \frac{T - T_s^{\mathrm{CW}}}{T - T_0}. \qquad (3)$$

The difference $T_s^{\mathrm{CW}} - T_0 = \lambda^2/AC_{66,0}$ (the "Jahn-Teller energy" of Refs. [20,21]) is an energy scale characteristic of the electron-lattice coupling.

In the following we extract the nematic susceptibility χ_φ from our data using the above Landau theory. We use the approximation $C_{66}/C_{66,0} \approx Y_{[110]}/Y_0$, where Y_0 is the noncritical background. For Y_0, we use 33%Co-Ba122 data [30], the temperature dependence of which can be very well described by the empirical Varshni formula [31] $Y_0 = c_0 - s/[\exp(t/T) - 1]$ with $s/c_0 = 0.0421$ and $t = 123.6$ K

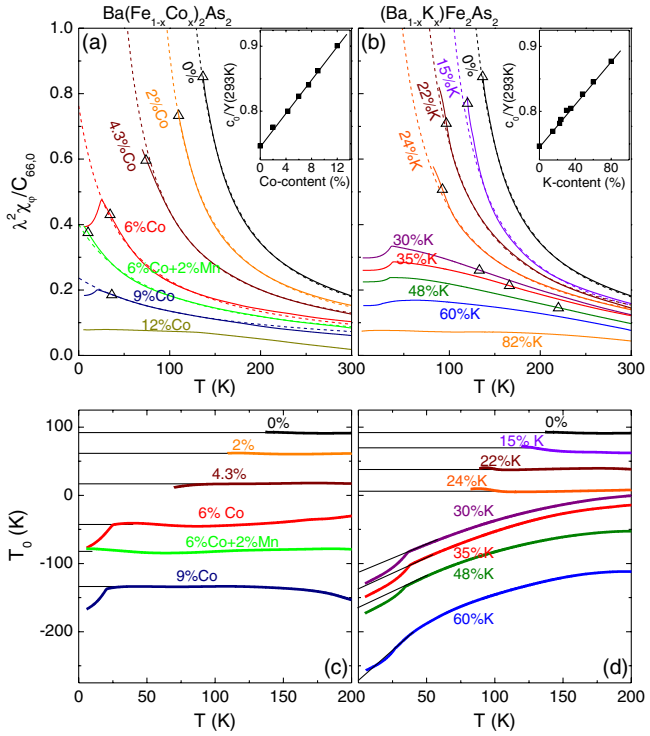

FIG. 2 (color online). Nematic susceptibility, χ_φ in units of $\lambda^2/C_{66,0}$, obtained from the critical part of the Young's modulus of (a) Co-Ba122 and (b) K-Ba122. Dashed lines correspond to a Curie-Weiss fit using Eq. (3). Insets show the parameter $c_0/Y_{[110]}(293\ \mathrm{K})$ used for separating the critical part of $Y_{[110]}$ from the background (see text for details). Triangles mark the inflection point of $\chi_\varphi(T)$, T^*, which is a lower temperature limit for its Curie-Weiss-like divergence. (c), (d) Temperature-dependent Curie-Weiss temperature $T_0(T) = 1 - 1/A\chi_\varphi$ of the nematic susceptibility for (c) Co-Ba122 and (d) K-Ba122. Linear extrapolations beyond the structural or superconducting transition are shown as thin black lines.

[see inset in Fig. 1(c)]. $c_0/Y(293\ \mathrm{K})$ remains a free parameter, because we lack absolute values of Y. The values of $c_0/Y(293\ \mathrm{K})$ were adjusted in order to obtain good agreement with Eq. (3) for the underdoped samples and then linearly extrapolated to higher doping levels (see insets of Fig. 2). Making use of Eq. (2), the normalized nematic susceptibility $\lambda^2\chi_\varphi/C_{66,0}$ can thus be obtained from our data [Figs. 2(a) 2(b)].

Figure 3(a) shows the magnitude of the nematic susceptibility χ_φ (in units of $\lambda^2/C_{66,0}$) as a color-coded map in the composition-temperature phase diagram of Co-Ba122 and K-Ba122. χ_φ is significantly enhanced in a broad band around the structurally distorted phase, as expected. It is largest for the undoped compound right above T_s and decreases smoothly with both electron and hole doping. This is at variance with Ref. [15], where a maximum of the nematic susceptibility around optimal doping has been reported. Importantly, the enhancement of χ_φ extends over most of the superconducting domes of both systems, even when no structural phase transition occurs. In fact, there appears to be a universal relationship between the ratio $T_c/T_{c,\max}$ [$T_{c,\max} = 25$ K (38 K) for Co-Ba122 (K-Ba122)] and the maximum value of $\chi_\varphi(T)$ for the overdoped samples of both systems [Fig. 3(b)]. If the nematic susceptibility is taken as a measure of the strength of nematic fluctuations, this suggests that these fluctuations may mediate the superconducting pairing also over the whole, rather wide, superconducting dome of K-Ba122.

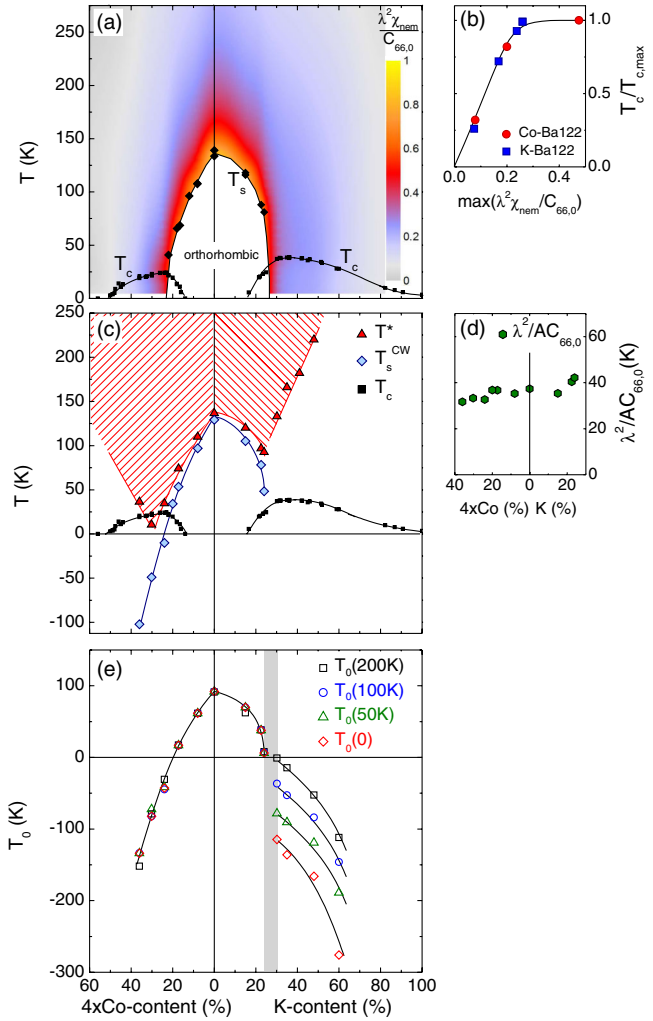

FIG. 3 (color online). (a) Temperature and doping dependence of the magnitude of the normalized nematic susceptibility $\lambda^2\chi_\varphi/C_{66,0}$ for Co-Ba122 and K-Ba122 from Fig. 2. (b) $T_c/T_{c,\max}$ as a function of the maximum value of $(\lambda^2\chi_\varphi/C_{66,0})(T)$ for all overdoped samples. (c) Phase diagram showing the doping dependence of T^*, T_s^{CW} and T_c. The red dashed area corresponds to the "critical" region above T^* where $\chi_\varphi(T)$ diverges. (d) Doping dependence of the electron-lattice coupling energy $T_s^{\mathrm{CW}} - T_0 = \lambda^2/AC_{66,0}$. (e) Curie-Weiss temperature T_0 at various temperatures obtained from Fig. 2(c) 2(d). An abrupt change from Curie-Weiss to non-Curie-Weiss behavior occurs in the shaded region. Lines are a guide to the eye.

In Fig. 2 we also show the results from a Curie-Weiss analysis of the nematic susceptibility. The dashed lines in Figs. 2(a) 2(b) show a fit of the data to Eq. (3), which takes the form $(\lambda^2\chi_\varphi/C_{66,0})(T) = (T_s^{\mathrm{CW}} - T_0)/(T - T_0)$. The resulting parameters are plotted in Figs. 3(c) 3(d). The coupling energy $T_s^{\mathrm{CW}} - T_0 = \lambda^2/AC_{66,0} \sim 30$–$40$ K is practically doping independent. In the electron-doped system, T_s^{CW} changes smoothly from positive to negative values, a behavior which has been associated with a QCP at optimal doping [21]. Note that the hole-doped system with K content $\geq 30\%$ cannot be described successfully by the simple Curie-Weiss law.

In order to study how hole-doped K-Ba122 differs from Co-Ba122, we define a lower temperature limit for the breakdown of the Curie-Weiss law by the inflection point of $\chi_\varphi(T)$, T^*. T^* has been marked in Figs. 2(a) 2(b), by open triangles and is also plotted in Fig. 3(c). As a function of doping, T^* first decreases, closely following T_s, and then increases upon further doping. The region of possible critical softening above T^* extents to near zero temperatures only in the electron-doped system, in agreement with a quantum critical scenario. Note that, in order to "look beneath" the superconducting dome, we used a nonsuperconducting 6%Co + 2%Mn-codoped sample, because Mn substitution strongly suppresses T_c but affects T_s only slightly [32]. In contrast, the values of T^* for the hole-doped system clearly do not go below ~75 K, which is incompatible with a QCP in this system. It is curious that optimally doped K-Ba122, the sample with the highest T_c, does not show Curie-Weiss-like critical softening. Note that also the hardening below T_c is significantly less pronounced in optimally doped K-Ba122 than in optimally doped Co-Ba122. For a detailed description of the anomalies at and below T_c, see [23].

In order to better quantify the deviations from the Curie-Weiss behavior, we ascribe them to a temperature dependence of the parameter T_0 in Eq. (3). $T_0(T)$ can be obtained from the data in Figs. 2(a) 2(b) assuming that no other parameter is temperature dependent, and that $\lambda^2/AC_{66,0} = 40$ K for K-Ba122 with $\geq 30\%$ K content. Figures 2(c) 2(d) show that $T_0(T)$ is temperature independent for Co contents up to 9% and K contents up to 24% confirming that the nematic susceptibility obeys the Curie-Weiss law for these compounds. In contrast, $T_0(T)$ is strongly temperature dependent for higher K contents. This contrasting behavior is made even more evident in Fig. 3(e) in which T_0 at different temperatures is plotted as a function of doping. A linear extrapolation is used for temperatures which lie below the structural or superconducting phase transitions. There is a clear abrupt change in behavior between 24% and 30% K content, above which T_0 is no longer constant and decreases with decreasing temperature below 200 K. Especially at low temperatures, a steplike anomaly of T_0 as a function of doping occurs, which we associate with a first order transition between magnetic (orthorhombic) and non-magnetic (tetragonal) ground states on increasing the K content. The decrease of T_0 with decreasing temperature shows that the tendency towards nematic ordering is weakened at lower temperature. Interestingly, a change of the topology of the Fermi surface from strongly nesting circular hole pockets to "propeller-shaped" hole pockets with expected weaker nesting has been found to occur on lowering the temperature in optimally doped K-Ba122 [33]. Such a change of topology of the Fermi surface could explain why T_0 becomes temperature dependent.

In conclusion, we have shown that the nematic susceptibility is enhanced over the whole superconducting regions in both K- and Co-doped Ba122, suggesting that fluctuations associated with the electronic nematic order possibly play a crucial role in superconducting pairing. On the other hand, nematic fluctuations exhibit quantum critical-like behavior only in Co-Ba122 and not in K-Ba122, which has the higher T_c. This naturally raises the question whether quantum criticality is really important for obtaining high T_c and/or if nematic fluctuations are indeed directly involved in the pairing. From our measurements alone it is impossible to determine whether nematic order is driven by spin or orbital physics. However, a comparison between the χ_φ presented here and the nematic susceptibility in the spin-nematic model (obtained from nuclear magnetic resonance measurements) was carried out for Co-Ba122 [34], providing strong evidence for a magnetically driven structural transition. Similar tests with K-Ba122 are highly desirable.

We thank Andres Cano, Rafael M. Fernandes, Jörg Schmalian, Kees van der Beek, and Bernd Wolf for valuable discussions. This work was funded by the DFG through SPP1458 and via a "Feasibility Study of Young Scientists" in the framework of the Exzellenz-Initiative at the KIT.

*anna.boehmer@kit.edu
†christoph.meingast@kit.edu

[1] M. R. Norman, Science **332**, 196 (2011).
[2] G. R. Stewart, Rev. Mod. Phys. **83**, 1589 (2011).
[3] C.-C. Lee, W.-G. Yin, and W. Ku, Phys. Rev. Lett. **103**, 267001 (2009).
[4] W. Lv, F. Krüger, and P. Phillips, Phys. Rev. B **82**, 045125 (2010).
[5] H. Kontani, T. Saito, and S. Onari, Phys. Rev. B **84**, 024528 (2011).
[6] S. Nandi, M. G. Kim, A. Kreyssig, R. M. Fernandes, D. K. Pratt, A. Thaler, N. Ni, S. L. Bud'ko, P. C. Canfield, J. Schmalian, R. J. McQueeney, and A. I. Goldman, Phys. Rev. Lett. **104**, 057006 (2010).
[7] R. M. Fernandes and J. Schmalian, Supercond. Sci. Technol. **25**, 084005 (2012).
[8] I. I. Mazin, D. J. Singh, M. D. Johannes, and M. H. Du, Phys. Rev. Lett. **101**, 057003 (2008).

[9] H. Kontani and S. Onari, Phys. Rev. Lett. **104**, 157001 (2010).
[10] K. Kuroki, S. Onari, R. Arita, H. Usui, Y. Tanaka, H. Kontani, and H. Aoki, Phys. Rev. Lett. **101**, 087004 (2008).
[11] I. I. Mazin and J. Schmalian, Physica (Amsterdam) **469C**, 614 (2009).
[12] J.-H. Chu, J. G. Analytis, K. D. Greve, P. L. McMahon, Z. Islam, Y. Yamamoto, and I. R. Fisher, Science **329**, 824 (2010).
[13] M. Yi, D. Lu, J.-H. Chu, J. G. Analytis, A. P. Sorini, A. F. Kemper, B. Moritz, S.-K. Mo, R. G. Morre, M. Hashimoto, W.-S. Lee, Z. Hussain, T. P. Devereaux, I. R. Fisher, and Z.-X. Shen, Proc. Natl. Acad. Sci. U.S.A. **108**, 6878 (2011).
[14] S. Kasahara, H. J. Shi, K. Hashimoto, S. Tonegawa, Y. Mizukami, T. Shibauchi, K. Sugimoto, T. Fukuda, T. Terashima, A. H. Nevimdomskyy, and Y. Matsuda, Nature (London) **486**, 382 (2012).
[15] J.-H. Chu, H.-H. Kuo, J. G. Analytis, and I. R. Fisher, Science **337**, 710 (2012).
[16] Y. Gallais, R. M. Fernandes, I. Paul, L. Chauvière, Y.-X. Yang, M.-A. Méasson, M. Cazayous, A. Sacuto, D. Colson, and A. Forget, Phys. Rev. Lett. **111**, 267001 (2013).
[17] S. A. K. E. Fradkin, M. J. Lawler, J. P. Eisenstein, and A. P. Mackenzie, Annu. Rev. Condens. Matter Phys. **1**, 153 (2010).
[18] M. Vojta, Adv. Phys. **58**, 699 (2009).
[19] R. M. Fernandes, L. H. VanBebber, S. Bhattacharya, P. Chandra, V. Keppens, D. Mandrus, M. A. McGuire, B. C. Sales, A. S. Sefat, and J. Schmalian, Phys. Rev. Lett. **105**, 157003 (2010).
[20] T. Goto, R. Kurihara, K. Araki, K. Mitsumoto, M. Akatsu, Y. Nemoto, S. Tatematsu, and M. Sato, J. Phys. Soc. Jpn. **80**, 073702 (2011).
[21] M. Yoshizawa, D. Kimura, T. Chiba, S. Simayi, Y. Nakanishi, K. Kihou, C.-H. Lee, A. Iyo, H. Eisaki, M. Nakajima, and S. Ushida , J. Phys. Soc. Jpn. **81**, 024604 (2012).
[22] C. Meingast, B. Blank, H. Bürkle, B. Obst, T. Wolf, H. Wühl, V. Selvamanickam, and K. Salama, Phys. Rev. B **41**, 11299 (1990).
[23] See Supplemental Material at http://link.aps.org/supplemental/10.1103/PhysRevLett.112.047001 for further experimental details and an analysis of the coupling between nematic susceptibility and superconductivity.
[24] A. V. Kityk, V. P. Soprunyuk, A. Fuith, W. Schranz, and H. Warhanek, Phys. Rev. B **53**, 6337 (1996).
[25] E. Salje, *Phase Transitions in Ferroelastic and Co-Elastic Crystals* (Cambridge University Press, Cambridge, England, 1990).
[26] W. Schranz, H. Kabelka, and A. Tröster, Ferroelectrics **426**, 242 (2012).
[27] W. Schranz, H. Kabelka, A. Sarras, and M. Burock, Appl. Phys. Lett. **101**, 141913 (2012).
[28] M. Yoshizawa and S. Simayi, Mod. Phys. Lett. B **26**, 1230011 (2012).
[29] A. Cano, M. Civelli, I. Eremin, and I. Paul, Phys. Rev. B **82**, 020408 (2010).
[30] C. Meingast, F. Hardy, R. Heid, P. Adelmann, A. Böhmer, P. Burger, D. Ernst, R. Fromknecht, P. Schweiss, and T. Wolf, Phys. Rev. Lett. **108**, 177004 (2012).
[31] Y. P. Varshni, Phys. Rev. B **2**, 3952 (1970).
[32] 2% Mn substitution decreases T_s equivalently to 0.7% Co substitution, A. E. Böhmer *et al.* (unpublished).
[33] D. V. Evtushinsky, A. A. Kordyuk, V. B. Zabolotnyy, D. S. Inosov, T. K. Kim, B. Büchner, H. Luo, Z. Wang, H.-H. Wen, G. Sun, C. Lin, and S. V. Borisenko, J. Phys. Soc. Jpn. **80**, 023710 (2011).
[34] R. M. Fernandes, A. E. Böhmer, C. Meingast, and J. Schmalian, Phys. Rev. Lett. **111**, 137001 (2013).